

Demonstration of the self-mixing effect in interband cascade lasers

K. Bertling, Y. L. Lim, T. Taimre, D. Indjin, P. Dean, R. Weih, S. Höfling, M. Kamp, M. von Edlinger, J. Koeth, and A. D. Rakić

Citation: [Applied Physics Letters](#) **103**, 231107 (2013); doi: 10.1063/1.4839535

View online: <http://dx.doi.org/10.1063/1.4839535>

View Table of Contents: <http://scitation.aip.org/content/aip/journal/apl/103/23?ver=pdfcov>

Published by the [AIP Publishing](#)

Articles you may be interested in

[A microchip laser source with stable intensity and frequency used for self-mixing interferometry](#)

Rev. Sci. Instrum. **87**, 053114 (2016); 10.1063/1.4947494

[High resolution quartz flexure accelerometer based on laser self-mixing interferometry](#)

Rev. Sci. Instrum. **86**, 065001 (2015); 10.1063/1.4921903

[Robust real-time self-mixing interferometric laser vibration sensor with embedded MEMS accelerometer](#)

AIP Conf. Proc. **1457**, 148 (2012); 10.1063/1.4730553

[Demonstration of a self-mixing displacement sensor based on terahertz quantum cascade lasers](#)

Appl. Phys. Lett. **99**, 081108 (2011); 10.1063/1.3629991

[Self-mixing interferometry in vertical-cavity surface-emitting lasers for nanomechanical cantilever sensing](#)

Appl. Phys. Lett. **94**, 091103 (2009); 10.1063/1.3086893

The advertisement for Goodfellow features a collage of various materials and components. On the left, there are several red and white pills. In the center, there are small metal parts and a blue component. On the right, there are various powders, granules, and a yellow component. The text is overlaid on the left side of the collage.

Pure Metals • Ceramics
Alloys • Polymers
in dozens of forms

Goodfellow

Small quantities *fast* • Expert technical assistance • 5% discount on online orders

Demonstration of the self-mixing effect in interband cascade lasers

K. Bertling,¹ Y. L. Lim,¹ T. Taimre,² D. Indjin,³ P. Dean,³ R. Weih,⁴ S. Höfling,⁴ M. Kamp,⁴ M. von Edlinger,⁵ J. Koeth,⁵ and A. D. Rakić^{1,a)}

¹*School of Information Technology and Electrical Engineering, The University of Queensland, Brisbane, QLD 4072, Australia*

²*School of Mathematics and Physics, The University of Queensland, Brisbane, QLD 4072, Australia*

³*School of Electronic and Electrical Engineering, University of Leeds, Leeds LS2 9JT, United Kingdom*

⁴*Technische Physik, Physikalisches Institut, Universität Würzburg and Wilhelm Conrad Röntgen Research Center for Complex Material Systems, Universität Würzburg, Am Hubland, D-97074, Würzburg, Germany*

⁵*nanoplus GmbH, Oberer Kirschberg 4, 97218 Gerbrunn, Germany*

(Received 15 October 2013; accepted 19 November 2013; published online 4 December 2013)

In this Letter, we demonstrate the self-mixing effect in an interband cascade laser. We show that a viable self-mixing signal can be acquired through the variation in voltage across the laser terminals, thereby removing the need for an external detector. Using this interferometric technique, we have measured the displacement of a remote target, and also demonstrated high resolution imaging of a target. The proposed scheme represents a highly sensitive, compact, and self-aligned sensing technique with potential for materials analysis in the mid-infrared. © 2013 AIP Publishing LLC. [<http://dx.doi.org/10.1063/1.4839535>]

Interband cascade lasers (ICLs) are a promising room temperature, continuous-wave (CW) source of narrowband mid-infrared (MIR) radiation.^{1–4} The recent availability of MIR ICLs has driven the development of new chemical sensing systems that make use of unique molecular spectroscopic signatures in the MIR.⁵ With envisaged applications in chemical analysis and biomedicine, MIR ICLs present a viable alternative to MIR quantum cascade lasers (QCLs) due to their much lower input-power requirements.^{1–4,6} Furthermore, high sensitivity MIR detectors usually require active cooling to be effective (and even cryogenic cooling at longer wavelengths).

These problems can be overcome by using an ICL as both the source and detector of MIR radiation by exploiting the self-mixing (SM) effect in these devices. With their input-power requirements almost two orders of magnitude lower than those now attainable for QCLs, ICLs are well positioned to become the lasers of choice for all applications which require long-term continuous-wave room temperature operation at relatively low output powers.^{1,4} The resulting SM system yields a low input-power, self-aligned compact sensor with coaxial optical geometry that can continuously operate at room temperature for extended periods of time.

The SM effect occurs when radiation emitted from the laser interacts with a distal target and part of the radiation is reflected back and injected into the laser cavity. This returned light causes perturbations to the operating parameters of the laser (such as the threshold gain, emitted power, lasing spectrum, and the laser voltage), thereby generating a measureable signal that contains information about the target.^{7,8} As such, a particularly convenient SM signal can be acquired by monitoring the voltage across the laser terminals. This permits the exploitation of the SM effect to create a simple, compact sensing system with high sensitivity and dynamic range.^{9–11} To date, SM sensors have been reported

for a wide range of laser wavelengths including visible, near-infrared, MIR, and recently terahertz.^{12–16}

In this Letter, we demonstrate the existence of the SM effect in ICLs. Further, using a MIR distributed feedback (DFB) ICL ($\lambda = 3.57 \mu\text{m}$) operating at room temperature, we demonstrate that the variation in voltage across the laser terminals caused by feedback can be used as a viable SM signal, thereby removing the need for an external detector. Our demonstration consists of two experiments. In the first experiment, we obtain a typical SM displacement signal from a target displaced along the optical axis of the system. Recalling the equivalence between displacement sensing and detecting temporal variations in the refractive index,¹⁷ it is clear that this system can also be used for measuring temporal changes in the refractive index of the medium located between the laser and the external reflector, or for measuring the refractive index of such a material.¹⁸ In the second experiment, we demonstrate an imaging system in the MIR using the SM effect in ICLs. This demonstrates the potential for imaging spatial (lateral) variations in refractive index or absorption of a target in the MIR range of the spectrum, following the procedure described in Ref. 19.

The DFB ICL that was used was fabricated on a GaSb substrate by molecular beam epitaxy. The waveguide structure consists of a lower ($3.5 \mu\text{m}$ thick) and an upper ($2 \mu\text{m}$ thick) InAs:Si/AlSb superlattice cladding with a 4.73 nm period. They sandwich two separate 200 nm thick GaSb:Te confinement layers which themselves surround the six stage active region. The cascade design was adapted from Ref. 1, since this structure with rebalanced carrier densities has proven to provide good lasing performance. To select a single longitudinal mode, deeply etched ridges with fourth order sidewall gratings were processed by e-beam lithography and dry etching. The operating characteristics (light-current curve and the emission spectrum) of the 0.9 mm long ICL used in this study can be seen in Fig. 1.

The experimental setup of the SM system is shown in Fig. 2. The ICL was kept at a constant temperature of $20 \text{ }^\circ\text{C}$

^{a)}rakic@itee.uq.edu.au

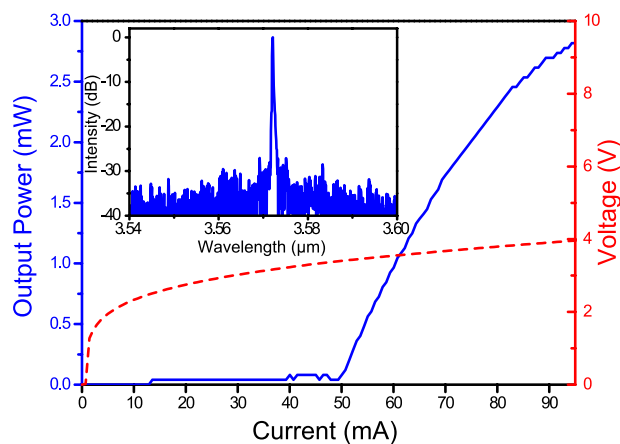


FIG. 1. Light-current (solid) and current-voltage (broken) characteristics of the MIR ICL. Inset: the emission spectrum of the MIR ICL at a drive current of 60 mA (at 20 °C).

using a Peltier effect based temperature controller mounted inside the laser package, and operated at a constant drive current of 65 mA. The emitted radiation from the ICL was collimated using a 2 in. diameter, 2 in. focal length off-axis parabolic reflector and focussed normally on the target using a second identical reflector (giving an optical path length of 341.6 mm). The beam was modulated at 1 kHz with an optical chopper placed just in front of the output aperture of the laser. Thus, the optical chopper modulates the optical feedback level the laser is experiencing. Two states are present: (1) chopper blade is obstructing the beam—laser is operating with virtually no feedback, and (2) the beam is transmitted between the blades and to the target—laser is operating with an external feedback level dictated by the target. These two states result in two distinct voltage levels across the ICL representing our SM (square-wave) signal in the time domain, shown in the inset to Fig. 2. The voltage signal was ac-coupled into a $\times 1000$ gain differential amplifier and subsequently fed into a 16-bit computer-based data acquisition card synchronised with the chopper. The target was mounted

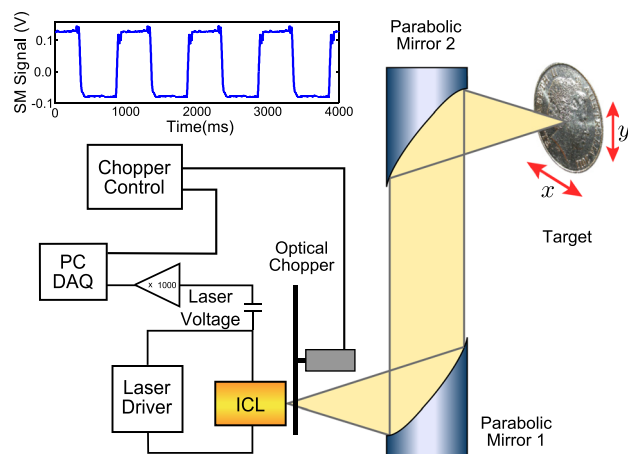


FIG. 2. Schematic diagram of the experimental apparatus used. The ICL was driven by a constant current (65 mA). An optical chopper was used to modulate the laser feedback. The ICL terminal voltage variations are acquired using an ac-coupled amplifier (with $\times 1000$ gain) and fed into a PC-based data acquisition card (PC DAQ). A pair of parabolic mirrors focuses the beam onto the remote target mounted on a computer-controlled three-axis translation stage. Inset: typical SM voltage signal acquired when optically chopping the laser beam (after amplification).

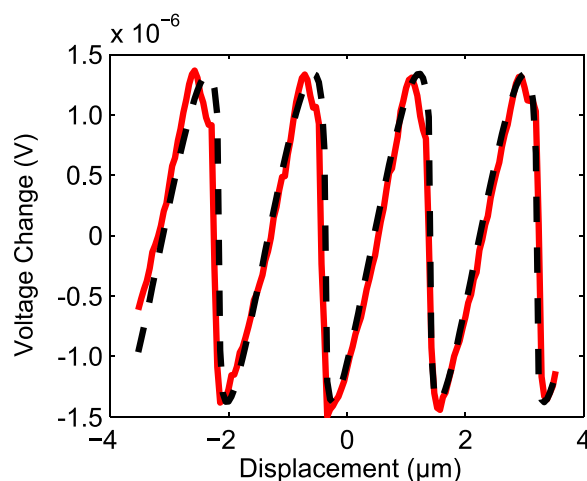


FIG. 3. Experimental RMS voltage signal (solid line) and fitted model (broken line) waveforms showing the typical interferometric fringes, as the chromium mirror is swept through the focal plane (at 0 μm displacement) of the second mirror.

on a three-axis computer-controlled translation stage, allowing it to be displaced along the optical axis of the system (z) or in a plane perpendicular to the optical axis (x - y).

This apparatus was used to perform the two experiments. In the first experiment, the target was displaced along the z -axis, thus creating a typical SM interferometric signal shown in Fig. 3. For this purpose, a chromium coated mirror was moved towards the laser, through the focal plane of the second mirror using the smallest step size achievable with our translation stage (47.625 nm). At each longitudinal step, the voltage signal across the laser was measured. Morphologically, the SM signal acquired in this way consists of a periodic square wave (see Fig. 2). The two voltage levels of the SM signal correspond to the two states of the optical chopper as explained earlier. The root-mean-square (RMS) voltage of this waveform was then computed and used to represent the strength of the SM signal. Figure 3 shows this measured SM signal strength as a function of distance (solid line) over relative displacement of $\pm 3.57 \mu\text{m}$ (± 1 wavelength) around the focal point of the second mirror. This waveform is typical of those observed for displacement experiments in other SM systems.^{16,20} The SM signal shows the four expected interferometric fringes for a total displacement of two wavelengths. Therefore, relative position of the target can be recovered from this SM signal with sub-wavelength resolution.²¹ The total amplitude change of the laser terminal voltage ($3 \mu\text{V}$ peak-to-peak) as the target is displaced is an order of magnitude smaller than the typical signal obtained for in-plane diode lasers or vertical-cavity surface-emitting lasers (which are both in the tens of microvolts^{22,23}) and several orders smaller than the terminal voltage change observed in terahertz QCLs (millivolts).^{19,24}

The experimental self-mixing waveform obtained in this way can be modelled through the use of the excess phase equation (that is, the steady-state solution to the Lang-Kobayashi rate equation model for a laser under optical feedback), when the stimulus is simply displacement linear in time.^{7,25} The broken line in Fig. 3 is the result of fitting this model to the experimental linear displacement data. From the model fit, we obtained an estimate for the feedback

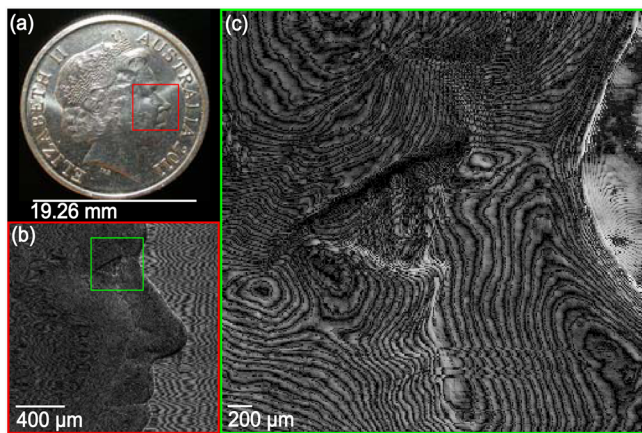


FIG. 4. Images generated from raster-scanning an Australian 5-cent coin. (a) Photograph of the coin. (b) Raster-scanned image obtained from the ICL voltage SM signal and with $10\ \mu\text{m}$ step size [area scanned shown as small square in (a)]. (c) Raster-scanned image obtained from the ICL voltage SM signal and with $5\ \mu\text{m}$ step size [area scanned shown as small square in (b)].

parameter²⁶ $C \approx 1$ from what is a highly reflective metallic target. This lends support to the idea that ICLs may be similarly stable under feedback, as has been reported for QCLs.²⁷

In the second experiment, a target with changing surface profile was imaged. In this case, the target was an Australian 5-cent coin. The target position was fixed longitudinally in the focal plane of the focusing mirror, and raster scanned in a plane perpendicular (x - y) to the optical axis (z). The voltage signal was acquired and processed exactly as in the displacement experiment, to produce a two-dimensional image. Figure 4 shows the results of two scans with different spatial resolution. The small square in Fig. 4(a) shows the $3 \times 3\ \text{mm}$ area scanned in $10\ \mu\text{m}$ steps, with the result of the scan shown in Fig. 4(b). The interference fringes in areas of the coin which are flat are particularly noticeable. When the step size was reduced to $5\ \mu\text{m}$, the fringes in areas with more rapid change in profile became readily visible [see Fig. 4(c)]. Each fringe is a line of constant height on the target, with height difference between two adjacent fringes corresponding to $\lambda/2$ ($\lambda/2 = 1.785\ \mu\text{m}$), giving an indication of the surface depth gradient, and suggesting the potential application of the SM technique to three-dimensional imaging.²⁸

In summary, we have demonstrated the SM effect in an ICL. We have shown that a SM signal in an MIR ICL can be acquired through the variation in voltage across the laser terminals, removing the need for an external detector. Using this SM system we have demonstrated measurement of longitudinal target displacements. Furthermore, we have demonstrated room-temperature, high-resolution, high-sensitivity imaging using an ICL, thereby opening up the possibility for imaging two-dimensional variations (mapping) of the refractive index or the absorption coefficient of biological and chemical samples at MIR wavelengths. In addition to being simple, compact and highly sensitive, our scheme offers the significant benefit of room temperature operation and very low input-power requirements. As we have demonstrated in earlier work, self-mixing sensors are most sensitive when operated close to the laser threshold.²⁴ With low threshold currents and low bias voltages (leading to input-power requirements almost two orders of magnitude lower than

those for QCLs) ICLs operated in CW at room-temperature are perfectly positioned to become the lasers of choice for MIR SM sensors. Our demonstration paves the way for the application of ICL-based SM systems to the identification or analysis of gases and materials at MIR wavelengths.

The authors acknowledge support of the European Cooperation in Science and Technology (COST) Action BM1205. This research was supported under Australian Research Council's Discovery Projects funding scheme (DP 120 103703) and the State of Bavaria. Y.L.L. acknowledges support under the Queensland Government's Smart Futures Fellowships programme. P.D. acknowledges support from the EPSRC (UK).

- ¹I. Vurgaftman, W. Bewley, C. Canedy, C. Kim, M. Kim, C. Merritt, J. Abell, J. Lindle, and J. Meyer, *Nat. Commun.* **2**, 585 (2011).
- ²R. Weih, M. Kamp, and S. Höfling, *Appl. Phys. Lett.* **102**, 231123 (2013).
- ³R. Weih, A. Bauer, M. Kamp, and S. Höfling, *Opt. Mater. Express* **3**, 1624 (2013).
- ⁴I. Vurgaftman, W. Bewley, C. Canedy, C. Kim, M. Kim, C. Merritt, J. Abell, and J. Meyer, *IEEE J. Sel. Top. Quantum Electron.* **19**, 1200210 (2013).
- ⁵J. Li, W. Chen, and H. Fischer, *Appl. Spectrosc. Rev.* **48**, 523 (2013).
- ⁶T. H. Risby and F. K. Tittel, *Opt. Eng.* **49**, 111123 (2010).
- ⁷R. Lang and K. Kobayashi, *IEEE J. Quantum Electron.* **16**, 347 (1980).
- ⁸J. Katz, S. Margalit, C. Harder, D. Wilt, and A. Yariv, *IEEE J. Quantum Electron.* **17**, 4 (1981).
- ⁹G. Giuliani, M. Norgia, S. Donati, and T. Bosch, *J. Opt. A, Pure Appl. Opt.* **4**, S283 (2002).
- ¹⁰T. Bosch, N. Servagent, and S. Donati, *Opt. Eng.* **40**, 20 (2001).
- ¹¹S. Donati, *Electro-Optical Instrumentation, Sensing and Measuring with Lasers* (Prentice Hall Professional Technical Reference, New Jersey, 2004).
- ¹²R. Kliese, Y. L. Lim, T. Bosch, and A. D. Rakic, *Opt. Lett.* **35**, 814 (2010).
- ¹³J. R. Tucker, A. D. Rakic, C. J. O'Brien, and A. V. Zvyagin, *Appl. Opt.* **46**, 611 (2007).
- ¹⁴J. von Staden, T. Gensty, W. Elsasser, G. Giuliani, and C. Mann, *Opt. Lett.* **31**, 2574 (2006).
- ¹⁵N. Kumazaki, Y. Takagi, M. Ishihara, K. Kasahara, A. Sugiyama, N. Akikusa, and T. Edamura, *Jpn. J. Appl. Phys., Part 1* **47**, 6320 (2008).
- ¹⁶Y. L. Lim, P. Dean, M. Nikolic, R. Kliese, S. P. Khanna, M. Lachab, A. Valavanis, D. Indjin, Z. Ikonic, P. Harrison, E. H. Linfield, A. G. Davies, S. J. Wilson, and A. D. Rakic, *Appl. Phys. Lett.* **99**, 081108 (2011).
- ¹⁷A. A. A. Bakar, Y. L. Lim, S. J. Wilson, M. Fuentes, K. Bertling, T. Taimre, T. Bosch, and A. D. Rakic, *Physiol. Meas.* **34**, 281 (2013).
- ¹⁸M. Fathi and S. Donati, *IET Optoelectron.* **6**, 7 (2012).
- ¹⁹A. D. Rakić, T. Taimre, K. Bertling, Y. L. Lim, P. Dean, D. Indjin, Z. Ikonic, P. Harrison, A. Valavanis, S. P. Khanna, M. Lachab, S. J. Wilson, E. H. Linfield, and A. G. Davies, *Opt. Express* **21**, 22194 (2013).
- ²⁰S. Donati, L. Falzoni, and S. Merlo, *IEEE Trans. Instrum. Meas.* **45**, 942 (1996).
- ²¹C. Bes, T. Bosch, G. Plantier, and F. Bony, *Opt. Eng.* **45**, 84402 (2006).
- ²²W. J. Burke, M. Eitenberg, and H. Kressel, *Appl. Opt.* **17**, 2233 (1978).
- ²³Y. L. Lim, K. Bertling, P. Rio, J. Tucker, and A. Rakic, *Photonics: Design, Technology, and Packaging II, Proc. SPIE Vol. 6038*, edited by D. Abbott, Y. S. Kivshar, H. H. Rubinsztein-Dunlop, and S. Fan (SPIE, 2006), pp. 60381O–1.
- ²⁴P. Dean, Y. L. Lim, A. Valavanis, R. Kliese, M. Nikolic, S. P. Khanna, M. Lachab, D. Indjin, Z. Ikonic, P. Harrison, A. D. Rakić, E. H. Linfield, and A. G. Davies, *Opt. Lett.* **36**, 2587 (2011).
- ²⁵P. Spencer, P. Rees, and I. Pierce, "Theoretical analysis," in *Unlocking Dynamical Diversity: Optical Feedback Effects on Semiconductor Lasers* (John Wiley & Sons, 2005), Chap. 2.
- ²⁶G. Giuliani and S. Donati, "Laser Interferometry," in *Unlocking Dynamical Diversity: Optical Feedback Effects on Semiconductor Lasers* (John Wiley & Sons, 2005), Chap. 7.
- ²⁷F. Mezzapesa, L. Columbo, M. Brambilla, M. Dabbicco, S. Borri, M. Vitiello, H. Beere, D. Ritchie, and G. Scamarcio, *Opt. Express* **21**, 13748 (2013).
- ²⁸P. Dean, A. Valavanis, J. Keeley, K. Bertling, Y. L. Lim, R. Alhathloul, S. Chowdhury, T. Taimre, L. H. Li, D. Indjin, S. J. Wilson, A. D. Rakić, E. H. Linfield, and A. G. Davies, *Appl. Phys. Lett.* **103**, 181112 (2013).